Volume 1 | Number 1 | Jan 2013 | Pages 1–100

Analyst

www.rsc.org/analyst

ROYAL SOCIETY OF CHEMISTRY

ROYAL SOCIETY OF CHEMISTRY

www.rsc.org/analyst

# Analyst

**ARTICLE TYPE**

# Plasmonic Aptamer-Gold Nanoparticle Sensors for Small Molecule Fingerprint Identification

**Jorge L Chávez[a], Juliann Leny[a,b], Suzanne Witt[a,c], Grant M. Slusher[a], Joshua A. Hagen[a] and Nancy Kelley-Loughnane[*a]**

The utilization of the plasmonic response of aptamer-gold nanoparticle conjugates (Apt-AuNPs) to design cross-reactive arrays for fingerprint identification of small molecular targets was demonstrated for the first time. Four aptamers with different structural features previously selected to bind different targets 10 were used in combination with AuNPs by adsorbing the DNA on the AuNPs surface. The optimized response of the Apt-AuNPs to the analytes showed that, depending on the specific aptamer used, target binding by the aptamer could result in an increase or decrease of Apt-AuNPs stability. These Apt-AuNPs showed the ability to recognize different analytes with different affinities, generating fingerprints that allowed unambiguous analyte identification with response times in less than fifteen minutes. Importantly, 15 it was observed that it was not necessary to select an aptamer per analyte of interest to generate differentiable signatures, but a subset of aptamers could be used to identify a larger number of analytes. The data was analyzed using principal component analysis, showing efficient clustering of the different datasets for qualitative and quantitative identification. This work opens the door to using these Apt-AuNPs in point of care diagnostics applications where fast sensors with easy to read outputs are needed.

## 20 Introduction

The design of sensors that detect different metabolites simultaneously with fast responses would improve the field of medical diagnostics and facilitate the development of personalized medicine[1]. Biomarker monitoring involves not only 25 the detection of specific targets, but more importantly, changes in their concentrations that could be indicative of specific health conditions.[2,3] Most of the efforts in sensor design are focused on systems that detect one target at the time with great selectivity and specificity[4,5]. However, when the goal is to characterize a 30 disease or the health status of an individual, monitoring the levels of multiple biomarkers simultaneously would provide a more complete characterization and potentially would result in better prognosis[6,7].

Applications requiring simultaneous monitoring of different 35 targets might benefit from sensors that interact with multiple analytes with different specificities[8]. In these multiplex systems, like the human nose and tongue, the identification of one compound is realized by the analysis of a target fingerprint with an array of sensors with cross-reactive responses to different 40 analytes[9,10]. Importantly, this sensing approach is less prone to result in false positives since the detection of a particular target is based on the response of multiple sensing units to the same target. When only one of the sensing elements failed resulting in false identification of an analyte, the error is easily noticed by the lack 45 of response of the other sensing elements to this analyte, since the probability of having all sensors failing simultaneously is very low[11].

Aptamers have shown great promise as biorecognition elements for biosensors providing great sensitivity and selectivity for a 50 wide range of analytes[12,13,14]. The ease of their chemical modification and their chemical and thermal stability made them valuable capture elements for sensor design[15]. It has been demonstrated that the sequence of certain aptamer clones can be optimized to tune their selectivity from one target to a family of 55 chemically related analytes. For instance, different clones of a cholic acid-binding aptamer were studied and a response to multiple hydrophobic steroids was observed by some of these clones[16]. Similarly, the well-known cocaine binding aptamer was mutated in specific positions close to the binding site to promote 60 binding to a series of steroids and create cross-reactive arrays[17]. In a different approach, SELEX has been modified by alternating the target a random pool of RNA was exposed to, achieving aptamer sequences that recognized the chemical core of a family of related compounds[18]. These examples show that the binding 65 properties of aptamers could be advantageous to design cross-reactive arrays[19].

Gold nanoparticles (AuNPs) have been used in a number of sensing approaches due to their colorimetric response to events that affect their stability[20,21]. Aptamers have been utilized with 70 AuNPs to create fast colorimetric sensors for different targets, ranging from ions[22] to small molecules[23,24,25] and proteins[26]. The

typical colorimetric assay with aptamers and AuNPs is based on the difference in affinity of AuNPs for single stranded DNA (*ss*-DNA) and double stranded DNA (*ds*-DNA). It has been demonstrated that *ss*-DNA adsorbed fast on the AuNPs surface, while AuNPs showed a much poorer affinity for *ds*-DNA[27]. In general, it has been proposed that target binding by an aptamer occurs with a conformational switch from a *ss*-DNA-like conformation in the absence of the target to a *ds*-DNA-like conformation after target binding[28]. Therefore, an aptamer exposed to a non-target analyte remained as *ss*-DNA and adsorbed on the AuNPs improving their stability due to the addition of negative charges to the AuNPs surface. On the contrary, an aptamer bound to its target, with a *ds*-DNA-like conformation, did not adsorb on the AuNPs and provided no improvement in stability. Experimentally, to detect a target with these sensors, an aptamer is exposed to the sample of interest and, after a short incubation time, AuNPs are added to the mixture. After the AuNPs and aptamer are allowed to interact, salt is added to test the stability of the AuNPs. The presence of the target and the formation of the *ds*-like DNA conformation after binding resulted in AuNPs aggregation with a color change to blue after salt addition (no DNA adsorption on AuNPs, no increase in stability). On the other hand, in the absence of the target, the AuNPs suspensions remained red (free aptamer adsorbed on the AuNPs, increased stability). We have observed when using this detection scheme, that a non-target analyte that remains free in solution after aptamer addition can potentially interact with the AuNPs surface affecting their stability, which resulted in false positives[29]. To prevent the non-specific interactions between unbound target and the AuNPs surface, the colorimetric assays used here involved aptamer adsorption on the AuNPs prior to target addition. These aptamer-AuNPs conjugates (Apt-AuNPs) were prepared by simply mixing the two components followed by buffer addition and an overnight incubation. The presence of the DNA prevented non specific interactions, while allowing a colorimetric response to the aptamer target, as reported previously by our group[29].

In the last few years, nanomaterials have been interfaced with bio-recognition elements (BREs) to design cross-reactive sensors for multiplex protein detection. The Rotello group has demonstrated nanoparticle-based cross-reactive sensing for identification of different types of proteins and cells with a fluorescence output[8, 30,31], and recently the plasmonic response of aptamer-modified nanorods to binding events was used for multiplexed protein detection[19]. Very recently, the use of the label-free plasmonic response of Apt-AuNPs in cross-reactive sensors for protein targets has been demonstrated[32,19]. Small molecular targets non-plasmonic multiplex detection based on aptamers has been recently demonstrated using fluorescence detection[33] and SERS[34]. However, the multiplex plasmonic identification of small molecular analytes has not been demonstrated to the best of our knowledge. Small molecules are challenging targets for cross-reactive sensors since they have lower number of functional groups compared to proteins, which makes their classification difficult.

In this work, we designed a library of Apt-AuNPs with four aptamers: adenosine binding aptamer (ABA)[35], riboflavin-binding aptamer (RBA)[36], estradiol-binding aptamer (EBA)[37] and cholic acid-binding aptamer (CABA)[38]. These analytes are biologically relevant biomarkers for different conditions: estradiol is an endocrine disrupting chemical, identified as a pollutant needed to be monitored to protect public health[37], adenosine is a component of many biological cofactors[38] and is a biomarker for renal injury[39], cholic acid is the main component of bile acids and is crucial for diagnosis of hepatobiliary diseases[40], riboflavin is essential for cell growth and development[41] and is used as a supplement in food[42]. Therefore, monitoring the levels of these compounds is important in a clinical setting. The colorimetric response of these Apt-AuNPs to their targets and the other analytes in this set was fully characterized. Importantly, while performing these studies an exciting phenomenon was observed: the effect of aptamer binding to its target on AuNPs stability depended on the aptamer used, and could result in an increase or decrease of particle stability. The aptamers used in this sensing scheme showed the ability to respond to multiple targets with different affinities. We demonstrated in this work that different fingerprints were obtained based on the combined response of the Apt-AuNPs to each of the analytes studied. Moreover, principal components analysis (PCA) was used to efficiently cluster the data, demonstrating that this library of Apt-AuNPs show great potential to be used as a cross-reactive arrays for multiplex detection of chemically similar molecules.

## Experimental Section

### Materials

Riboflavin, 17-β-estradiol, hydrogen tetrachloroaurate(III) (HAuCl$_4$), sodium citrate, sodium chloride (NaCl) , magnesium chloride (MgCl$_2$), cholic acid, adenosine, tris-HCl and potassium chloride (KCl) were obtained from Sigma-Aldrich (St. Louis, MO). HEPES buffer was purchased from Amresco Inc. (Solon, OH) All chemicals were of analytical grade and used without further purification.

### DNA Synthesis

All synthesis reagents were purchased from Glen Research (Sterling VA 20164), except where noted. All oligonucleotides were synthesized in-house using the following protocol: The phosphoramidite method of oligonucleotide synthesis was performed on an ABI 394 eight column DNA/RNA Synthesizer. Sequences were grown from a 3' end solid support base followed by a standard progression of 1) oxidation (washing with 0.02M I$_2$ in THF/Pyridine/H$_2$O); 2) detritylation (washing with 3% TCA/DCM) 3) coupling (introducing appropriate T,A,C, or G phosphoramadite) 4) capping (THF/Pyridine/Ac$_2$O) and 5) a final oxidation step to remove trace H$_2$O from the reaction chamber. For de-protection and purification, the glass beads attached to the base of the newly formed DNA were transferred to the bottom of a 25 mL glass test tube. Then 3 mL of a 1:1 Ammonium Hydroxide:Methylamine (Sigma-Aldrich St. Louis MO) solution was added to the tube. The tube and its contents were incubated at 65 °C for 30 min. After removal from the incubator 250 μL of 3M NaCl was pipetted into the mixture and vortexed briefly. Ice cold ethanol was added in 6 mL aliquot and the mixture was placed in the freezer for 30 min. After the sample test tube was removed the mixture was applied to a NAP-5 desalting column (GE Healthcare Bio-Sciences Pittsburgh, PA 15264) in 1 mL

fractions. Fractions were collected in 1.5 mL micro centrifuge tubes and concentrated using an Eppendorf Vacufuge (Eppendorf Hauppauge, NY 11788). Samples were then re-suspended to working concentrations using DNAse free $H_2O$.

### AuNPs Synthesis and Characterization

The AuNPs were synthesized as reported previously[24]. In brief, 98 mL of deionized water (Millipore, Billerica,MA) were mixed with 2 mL of 50 mM $HAuCl_4$, heated and refluxed. As soon as reflux started, 10 mL of a 38.8 mM sodium citrate solution was added. The solution turned red after a few minutes. Heat was discontinued and the reaction was allowed to continue for 20 min under constant stirring. Subsequently, the suspension was allowed to cool down and filtered with a 0.2 µm polyester membrane. The AuNPs suspensions were kept in the dark when not in use at RT. The AuNPs size was determined to be 15 nm by dynamic light scattering (DLS). The extinction maximum was determined to be 520 nm in a Cary 300 UV spectrophotometer (Agilent Technologies, Santa Clara, CA). The AuNP concentration was calculated to be 10 nM, based on a molar absorption coefficient of $2.4 \times 10^8$ L mol$^{-1}$ cm$^{-1}$.

### Assay Design

AuNP-aptamer conjugates (80 aptamers per AuNP) were prepared by mixing 2 mL 10 nM AuNPs (15 nm) with 16 µL of 100 µM DNA. These mixtures were allowed to incubate for at least 2 hours and then were diluted 1:1 with 10 mM HEPES, 1 mM $MgCl_2$ buffer. This mixture was then left to incubate overnight. The Apt-AuNPs were typically used within three days after their preparation. In the case of the ABA- and EBA-AuNPs, the first step in the assay optimization was to determine the NaCl needed to promote a mild aggregation of the AuNPs exposed to a blank sample. Once the NaCl concentration was set, the same experiment was performed with a sample containing the aptamer's target (adenosine for ABA and estradiol for EBA). A higher aggregation response was observed in the presence of the target in each case. The NaCl concentration was adjusted again to maximize the difference in response between the blank and the target-containing samples. Finally, the linear range of the response was determined and each analyte was tested in this concentration range with the other Apt-AuNPs. In the case of CABA and RBA, the Apt-AuNPs were exposed to NaCl concentration that promoted severe aggregation, since preliminary data showed that target binding increased the Apt-AuNPs stability. Once the optimal NaCl concentration to promote Apt-AuNPs aggregation in the presence of a blank was determined, similar experiments were performed in the presence of the target, followed by assay optimization.

### Analyte Detection

To prepare the targets, a 100 mM stock solution of adenosine, estradiol, and cholic acid and a 10 mM stock solution of riboflavin were made by dissolving the analytes in dimethyl sulfoxide. Then each target was diluted down with the appropriate buffer to the concentrations reported in the plots. Estradiol and adenosine were diluted using a 1/3 Strength Estradiol Binding Buffer (33.3 mM Tris-HCl, 66.7 mM NaCl, 8.3 mM KCl, 3.3 mM $MgCl_2$, 1.7% EtOH). Riboflavin and cholic acid were diluted using the 10 mM HEPES, 1 mM $MgCl_2$ buffer.

AuNPs (75 µL) were mixed with 10 µL of the analyte stock solution. The mixtures were incubated for 10 min in a 96-well plate, protected from light. Subsequently, a volume of a 2 M NaCl solution was added simultaneously to all the wells used in an experiment to obtain the same final salt concentration. After briefly mixing the samples, the plate was immediately transferred to a Spectra Max M5 plate reader (Molecular Devices, Sunnyvale, CA) and the extinction of the AuNP suspensions at 530 and 650 nm was recorded. The degree of aggregation was plotted as the ratio of the extinction intensity of the aggregated AuNPs (extinction at 650 nm) over the individual AuNPs (extinction at 530 nm) as a function of target concentration.

### Principal Component Analysis

For PCA analysis, five replicates of the response of each Apt-AuNP to each analyte at a concentration of 15 and 20 µM were obtained. The data was analyzed with XLSTAT software.

## Results and Discussion

### Apt-AuNP Library Design

Four aptamers reported in the literature were selected to design Apt-AuNPs by the following criteria (see Table 1 for sequences): they bind to small molecules with relatively similar structures (see Figure 1A for chemical structures), they have different lengths, and their predicted secondary structures are significantly different (See Figure 1B for a schematic representation of their conformations and Figure S1 for mfold predicted structures). The use of aptamers with different structural features was intended to increase the probability of having different interactions between each analyte and the different aptamers, increasing the chances of obtaining fingerprints. Using analytes with relatively similar structures but that do not belong to the same family, was expected to provide a means to study the cross-reactivity of these Apt-AuNPs.

It is important to consider that the selectivity and affinity of the aptamer free in solution could be affected by aptamer immobilization on a surface. In the case studied here, the aptamers are adsorbed on the AuNPs surface, interacting strongly with the AuNPs through the interaction of multiple nucleotides, which could alter target binding thermodynamics and kinetics. In this work, the DNA and AuNPs were combined at a nominal ratio of 80:1. Due to the differences in the structures and lengths of the aptamers used, it can be anticipated that each aptamer might have different affinities for the AuNPs surface, which might result in differences in the number of DNA strands actually deposited on the AuNPs surface. The Apt-AuNPs were not purified to separate free and adsorbed DNA, due to the following reason: DNA adsorption on AuNPs involves an equilibrium between adsorbed and free species[43]. Since the DNA strands are only adsorbed on the AuNPs and not chemically attached, centrifugation of the Apt-AuNPs would promote removal of the free DNA, which would result on the release of more DNA to reach a new equilibrium. This process would end up in depletion of DNA from the AuNPs surface and with AuNPs with minimal stability.

### Effect of Analyte Adsorption on Citrate-Stabilized AuNPs Stability

**Table 1** Sequences of the aptamers used in this study

| Name | Sequence |
|------|----------|
| ABA | ACCTGGGGGAGTATTGCGGAGGAAGGT |
| EBA | GCTTCCAGCTAATTGAATTACACGCAGAGGGTAGCGGCTCTG CGCATTCAATTGCTGCGCGCTGAAGCGCGGAAGC |
| CABA | GCAGGGTCAATGGAATTAATGATCAATTGACAGACGCAAGTC TCCTGC |
| RBA | TTTTTTTTTTGGAACGACGGTGGTGGAGGAGATCGTTCC |
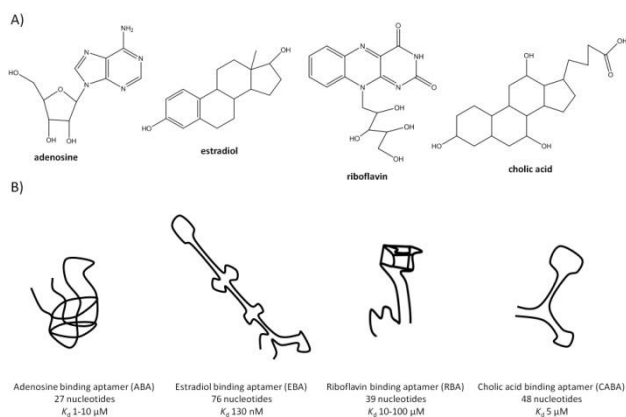


**Fig. 1** A) Chemical structures of analytes used in this study, B): Schematic representation of the experimentally reported structures of the aptamers used here, (see Figure S1 for mfold predicted structures).

It is well-known that different species with amine and hydroxyl groups, especially proteins, interact strongly with the surface of citrate-stabilized AuNPs[44,45]. Their adsorption on AuNPs can result in an increase or decrease in the AuNPs tendency to aggregate in media with high ionic strength, depending on the functional groups and structure of each protein. Figure S2 shows that the small molecule analytes used here interacted strongly with the AuNPs, as well. The plot shows the citrate-stabilized AuNP degree of aggregation: the ratio of AuNPs extinction at 650 nm (blue, aggregated AuNPs) and 530 nm (red, well-dispersed AuNPs), in the presence of each analyte (180 μM) before and after salt addition. It was observed that addition of adenosine, estradiol and riboflavin resulted in AuNPs aggregation when NaCl was added, while cholic acid resulted in AuNPs stabilization against salt-induced aggregation. The reason for the "stabilization" effect showed by cholic acid is difficult to explain, due to the similarity of its chemical structure to that of the other compounds. This is an example of how complex the system is, even when only two components are mixed, namely, the AuNPs and one analyte. Due to this, it was decided that to help prevent non-specific interactions between the analytes and the AuNPs, the DNA aptamers were going to be deposited on the AuNPs surface *before* analyte detection, as discussed next.

**Colorimetric Sensing with Apt-AuNPs**

The aptamer was allowed to adsorb on the AuNPs by an overnight incubation to prevent non-specific interactions between the surface-active analytes and AuNPs, as we have demonstrated previously[29]. The resulting Apt-AuNPs showed improved stability against salt-induced aggregation compared to the AuNPs non-exposed to the DNA, as observed by the higher NaCl concentration needed to obtain a change in color from red to blue.

Importantly, the amount of NaCl needed to promote the Apt-AuNPs aggregation was different for each aptamer, despite the fact that all aptamers were loaded at the same density: 80 aptamer/AuNP and they were all suspended in the same buffer. This was interpreted as evidence that each aptamer interacted differently with the AuNPs, probably due to a combination of the different aptamer lengths and structures. The first step in this work was to characterize the response of each Apt-AuNP to the four analytes studied here. In the first step, an aptamer was chosen to prepare Apt-AuNPs and the conjugates were exposed to the aptamer's target to determine the dynamic range of the response. The NaCl concentration needed to promote Apt-AuNPs aggregation was optimized independently for each Apt-AuNPs. In the second step, the same analyte was used to test the other Apt-AuNPs in the analyte concentration range determined in the first step. This protocol was repeated consistently for each Apt-AuNP-target sets. Each data set in a graph is normalized to the value of the blank for ease of comparison. Importantly, in all cases, the response of these Apt-AuNPs was obtained after ten minute incubation with the target followed by two minute incubation with salt, showing promise to develop fast colorimetric sensors. The variance of the data is shown in the graphs as the standard deviation of three replicates.

The response obtained with Apt-AuNPs made with the adenosine-binding aptamer (ABA-AuNPs) is shown in Figure 2A and B. The ABA is a short sequence that has been shown to form an extended pseudohelix in the binding complex that accommodates two adenosine molecules[46]. The ABA-AuNPs showed the typical response for this type of colorimetric assays, a large aggregation response in the presence of adenosine with minimal response to non-target analytes. This confirms that the DNA adsorption on the AuNPs surface prevented non-specific interactions between the AuNPs and the other analytes. Figure S3 shows TEM images of the ABA-ANPs exposed to buffer (Figure S3A) and adenosine (Figure S3B) after NaCl addition, confirming that the colorimetric response observed was due to AuNPs aggregation triggered by the target binding. The Apt-AuNPs designed with the estradiol binding aptamer (EBA-AuNPs) on the other hand, showed a large response to estradiol and riboflavin, a milder response to adenosine and no response to cholic acid, as shown in Figure 2C and D. The reason for this lack of selectivity is not clear yet. The EBA is the longest aptamer used here, with long stretches of paired nucleotides and four small loops[37], as shown schematically in Figure 1A (see Figure S1, for mfold prediction). We hypothesized that this lack of selectivity could be due to: i) interactions between the aptamer and the AuNPs surface that affected the aptamer conformation, and/or ii) the lack of strong interactions between the paired nucleotides and the AuNPs surface, which allowed analyte adsorption and resulted in significant cross-reactivity. In any case, both Apt-AuNPs followed the typical response observed when aptamers are used with AuNPs, a decrease in their stability against salt-induced aggregation after target binding by the aptamer, as shown schematically in Figure 2E. This was confirmed by DLS analysis of the change in the EBA-AuNPs size before and after salt addition in the presence and absence of the target. Table S1 shows Apt-AuNPs with hydrodynamic diameter of ~33 nm when exposed to assay buffer and salt, with the size

increasing to ~ 60 nm in the presence of estradiol under the same conditions. It is proposed that target binding resulted in the aptamer adopting a conformation that resembled ds-DNA, minimizing the interactions between the aptamer and the AuNPs
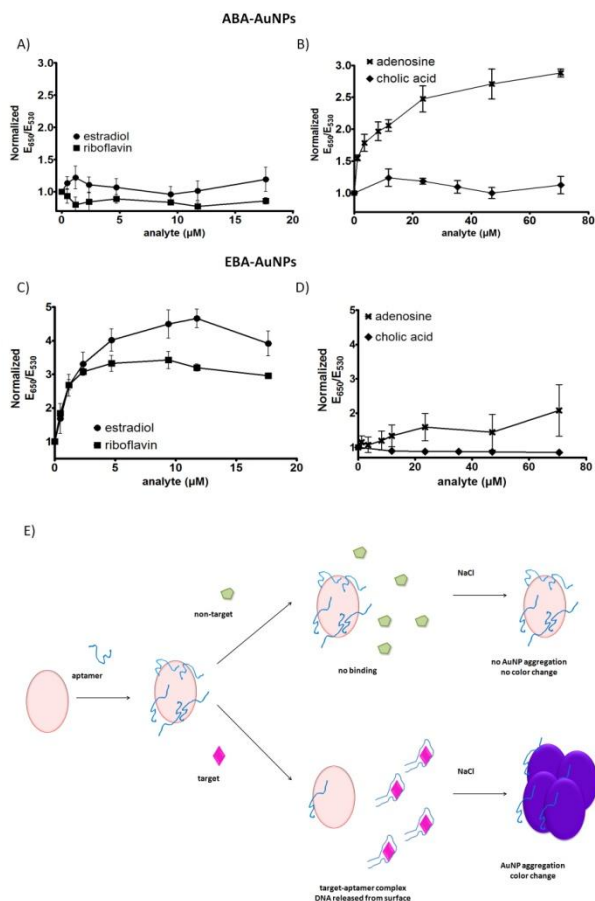


Fig. 2 Characterization of Apt-AuNPs cross-reactivity to different analytes. A) and B): ABA-AuNPs in 424 mM NaCl, data obtained two minutes after NaCl addition, C and D): EBA-AuNPs in 150 mM NaCl, data obtained two minutes after NaCl addition; data show the standard deviation of three replicates, E: proposed response mechanism.

surface. It is suggested that the more rigid *ds*-DNA cannot rearrange its nucleotide orientation to maximize favourable interactions between the nucleotides nitrogen atoms coordinating to the AuNPs surface[27]. As a result, the Apt-AuNPs became less stable and were more prone to salt-induced aggregation, compared to Apt-AuNPs exposed to non-target analytes or a blank.

The CABA-AuNPs did not respond to any analyte when they were tested in the same format as the ABA- and EBA-AuNPs, namely, they did not show a larger aggregation degree in the presence of cholic acid after NaCl addition, compared to the blank. Using increasing concentrations of salt in the assay to promote severe aggregation of the CABA-AuNPs suggested that cholic acid binding by the CABA-AuNPs resulted in an increased stability of the conjugates, compared to the controls. It is important to note that the assay optimization in this case is different from the assay discussed in the previous section. The CABA-AuNPs were exposed to NaCl concentrations that promoted their aggregation in the absence of any analyte. These same conditions were used in the presence of cholic acid and the other analytes. As shown in Figure 3A and B the CABA-AuNPs responded to cholic acid, with negligible responses to all non-target molecules. It could be argued that the response observed was due to cholic acid adsorption on the AuNPs without aptamer binding, however, the fact that there was no effect observed with adenosine even at high concentrations suggested that surface passivation by aptamer adsorption was optimal and prevented non-specific interactions. Figure S4 in the supplementary information shows TEM images of CABA-AuNPs exposed to buffer (Figure S4A) and cholic acid (S4B). The images showed that the colorimetric response reported is, in fact, due prevention of AuNPs aggregation due to cholic acid binding. This was further confirmed by DLS analysis of the size changes due to the addition of the NaCl in the presence and absence of cholic acid. The CABA-AuNPs exposed to the blank prior to salt addition showed a large hydrodynamic diameter (~181 nm), while in the presence of cholic acid under the same conditions, their size was ~48 nm, confirming the stabilizing effect of cholic acid binding by the aptamer (see Table S1).

Interestingly, target binding-induced Apt-AuNPs stability has previously been observed with the riboflavin aptamer. We have reported the design of RBA-AuNPs that responded to riboflavin at sub- micromolar levels with no response to 2-quinoxaline carboxylic acid (QCA), the chemical used in the negative selection step during SELEX[24]. As shown in Figure S2, riboflavin adsorption on citrate-stabilized AuNPs promoted AuNPs aggregation, therefore, analyte adsorption can be ruled out as the cause of the observed increased stability after riboflavin binding. The RBA-AuNPs showed an interesting case in which target adsorption on the AuNP surface promoted AuNP aggregation in the presence of salt but analyte binding by the Apt-AuNPs promoted AuNPs stability. It could be expected that these opposite effects would offset each other, resulting in minimal or very weak response to the target. The observed plasmonic response seemed to suggest that when the target was added there was a competition between the AuNPs surface and the aptamer for analyte binding. The net stabilization effect observed suggested that the aptamer had a higher affinity for the target than the analyte for the AuNP surface; therefore, the analyte was mainly bound to the aptamer, resulting in AuNPs stabilization. In this study, we expanded the RBA-AuNPs response characterization by exposing them to the other analytes. Figure 3C and D shows that a response to cholic acid was observed, with no responses to estradiol or adenosine, again confirming that non-specific analyte-AuNPs interactions were prevented.

Figure 1A and S1 shows that the CABA adopts a three-way junction structure, similar to the well-studied cocaine binding aptamer[47] (CoBA), while the RBA adopts the well-characterized G-quartet conformation. It is important to notice that our work shows that two aptamers with significant different structural features provided extra stability to the AuNPs upon target binding (RBA and CABA), while two aptamers with similar structures showed the opposite stabilization effect (CABA promoted increase in stability while CoBA resulted in decreased stability). These results seemed to indicate that the type of responses obtained with Apt-AuNPs cannot be predicted only by analyzing the aptamer structure. The exact reason for an aptamer to promote
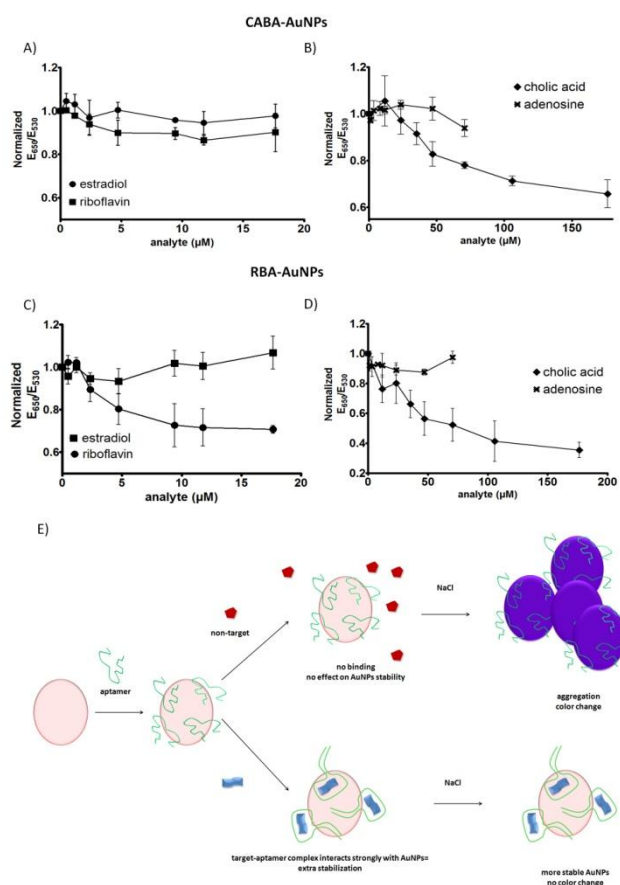
**Fig. 3** Characterization of Apt-AuNPs cross-reactivity to different analytes. A) and B): CABA-AuNPs in 370 mM NaCl, data obtained two minutes after NaCl addition, C and D): RBA-AuNPs in 333 mM NaCl, data obtained two minutes after NaCl addition; data show the standard deviation of three replicates, E: proposed response mechanism.

or prevent salt-induced aggregation in the Apt-AuNPs upon target binding is not clear yet, but we hypothesized that is a combination of complex surface-aptamer, target-aptamer, and target-surface interactions. This phenomenon is currently under investigation in our group. Importantly, this target binding-induced AuNP stability enhancement resembles what has been reported for thiol-anchored aptamers on AuNPs[48]. In this case, since the aptamers were covalently bound to the AuNPs surface, they could not be released upon target binding. It was proposed that the more compact aptamer-target complex formed on the AuNPs surface improved AuNPs stability by increasing the surface charge density near the AuNPs surface. We believe a similar mechanism is responsible for the effect observed here, as shown schematically in Figure 3E. We suggest that in this response mechanism, the DNA adsorbs on the AuNPs in a loose conformation covering less of the AuNPs surface, which might not provide optimal protection to the AuNPs from salt-induced aggregation. Upon target binding, a more compact structure is adopted increasing the charge density on the proximity of the AuNPs surface, resulting in higher particle stability. The data from these four Apt-AuNPs suggested that minimizing direct surface-analyte interactions was not enough to prevent responses to non-target analytes. While these responses to non-targets could be seen as a weakness of these colorimetric sensors, it has been

shown that sensors that respond to multiple targets with *different* affinities can be used to create cross-reactive sensors that mimic the human nose and tongue. Based on this concept, we analyzed the data of all sensors combined per target, as shown in Figure 4, to determine if these Apt-AuNPs could be used as cross-reactive sensors, as will be discussed in the next section.

**Plasmonic Fingerprint Analysis**

Cross reactive sensors try to mimic the human nose by detecting targets using a number of sensing subunits that respond with different affinities to different analytes. Ideally, when the output of each sensor subunit is combined, a unique fingerprint for each target is obtained. Most of the literature dealing with nanomaterials-based cross reactive arrays has focused on the identification of protein or cellular targets. This is due to the large number of functional groups present in these species, which improves the possibilities of observing different responses to each analyte with a cross reactive array. Small molecules on the other hand, due to their lower number of functional groups, are more challenging analytes, which required sensors with more powerful discrimination capabilities. Aptamers, due to their complex structural features have been shown to differentiate between analytes with similar chemical structures, showing promise for small molecule fingerprint identification. Analysis of our results suggested that a qualitatively different fingerprint for each analyte studied here could be generated by combining the response of each Apt-AuNP to the same target (Figure S5). The data shows that the cholic acid and adenosine fingerprints are easy to identify (Figure S5A and B, respectively). However, the fingerprints obtained for riboflavin and estradiol looked similar at first (Figures S5C and D, respectively), due to the dominant response given by the EBA-AuNPs (green bars). Notably, the fact that two different mechanisms of response were observed, allowed to clearly identify each target, as shown in the insets in the fingerprint plots for riboflavin and estradiol.

Importantly, the analyte fingerprints allowed not only their qualitative identification but detailed analysis of the data showed that analyte quantification was possible as well. As shown in Figure 4A, a different fingerprint was obtained with each target at the different concentrations tested. For clarity of comparison, the Apt-AuNPs response to the analytes at 15 and 20 μM (five replicates) was plotted side-by-side (Figure 4A), showing that the fingerprint "shape" was analyte concentration-dependent. From the point of view of simplicity of sensor design, it is preferred to use the minimum number of sensors units that provide enough discrimination power to identify the analytes of interest. Moreover, since aptamer selection could be a time consuming process and often quite challenging to implement for small molecule targets, it would be ideal to utilize the minimum number of aptamers to detect the larger number of analytes possible. To test this idea, we compared the fingerprint generated with the original four Apt-AuNPs and three Apt-AuNPs, after removing the data from the ABA-AuNPs, which was the least cross-reactive sensor. It was clearly observed that the discrimination power of the cross-reactive sensors was maintained when only three Apt-AuNPs were used, as observed by the different fingerprints obtained at both concentrations
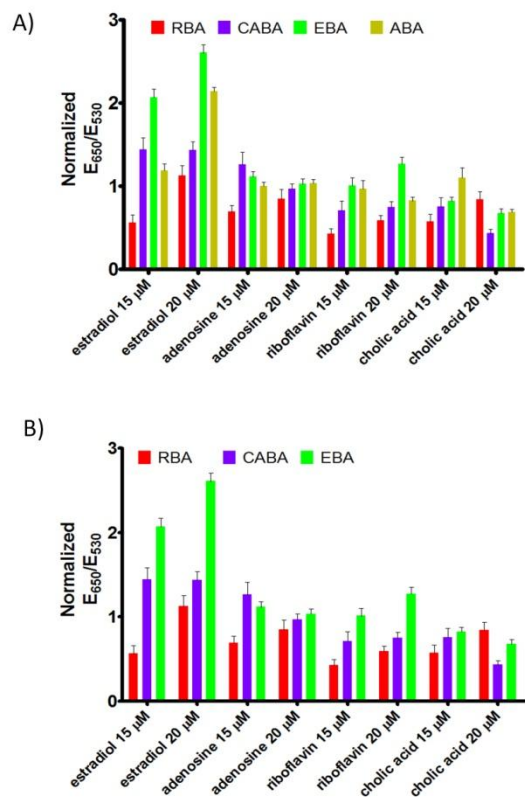
**Fig. 4** Fingerprint-based analyte identification at different concentrations. Comparison of the fingerprints obtained with analytes concentrations of 15 and 20 µM using: A) Four Apt-AuNPs, and B) Three ₅ Apt-AuNPs (after removal of the ABA-AuNPs data, the least responsive of the sensors). Error bars show the standard deviation of six replicates.

analyzed (Figure 4B). Moreover, the response of each Apt-AuNP to the two concentrations tested for each analyte was analyzed using the t-test. It was observed that, in most cases, a statistically ₁₀ different response was observed, Figure S6.

Visual identification and quantification of analytes fingerprint could be a tedious process. To simplify the data analysis from these cross-reactive sensors, a training set was obtained to determine whether principal components analysis (PCA) could be ₁₅ used to perform the analyte identification. To do this, five replicates of each data set were obtained per analyte studied at a concentration of 15 and 20 µM, resulting in a 5x4x9 matrix (five replicates, four sensors, and nine samples-one buffer and each analyte at two different concentrations-, the raw data is shown in ₂₀ Table S2). The Apt-AuNPs responses to the analytes studied were analyzed using PCA (see results in Table S3). Four canonical factors were obtained, with F1 (66.42%) and F2 (22.23%) accounted for most of the data variation (88.66%). Figure 5A, shows a PCA score plot using F1 and F2. Importantly, each ₂₅ analyte resulted in a different cluster that could be used for qualitative identification. Moreover, different concentrations of the same target resulted in different clusters, suggesting that these Apt-AuNPs could potentially be used for analyte quantification as well. The response of three Apt-AuNPs (without the ABA-₃₀ AuNPs, the least cross-reactive sensor) was analyzed by PCA as
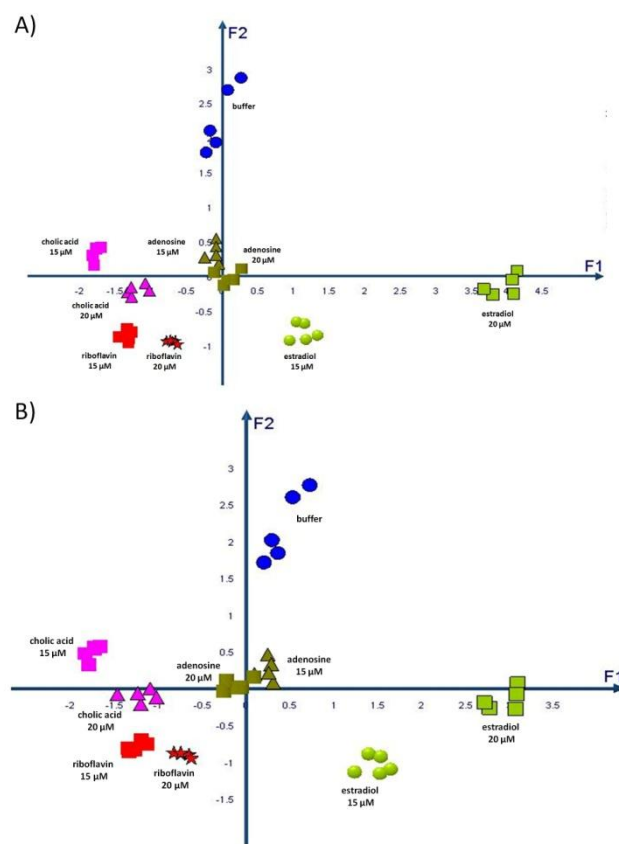


**Fig. 5** Principal Components Score Plot. The Apt-AuNPs response to the analytes of interest was analyzed by PCA, the sample set contained one ₃₅ buffer (blank) and each analyte at two concentrations: 15 and 20 µM. Analysis of data generated by A) the four Apt-AuNPs and B) three Apt-AuNPs (without the ABA-AuNPs data).

well, Figure 5B (see PCA output on Table S4 in the Supporting Information). Three canonical factors were obtained with F1 ₄₀ (66.01%) and F2 (29.14%) accounting for most of the variability (95.16%). It was observed that the three sensor matrix offered an optimal discrimination power, showing different clusters per each analyte at each concentration tested. In fact, no loss in the data resolution was observed when reducing the sensor matrix from ₄₅ four to three Apt-AuNPs. T-test analysis of the results showed that in all cases the outputs obtained for each analyte at the two concentrations tested were statistically different, see Figure S6 D. As discussed in the previous section, this data suggested that an aptamer for each analyte of interest is not necessary to create ₅₀ cross-reactive sensors, rather, it seems that a combination of a few aptamers with broad selectivities provide enough discrimination power for analyte sensing. Currently, we are exploring larger analyte sets with Apt-AuNPs libraries of different sizes to identify the minimum number of Apt-AuNPs ₅₅ necessary to identify a fixed number of targets.

## Conclusions

In this work, we designed Apt-AuNPs with aptamers that bind small molecules. Colorimetric assays for each target were

optimized and tested against multiple targets to determine whether these sensors show any cross-reactivity. Importantly, during these studies two different types of responses of the Apt-AuNPs to the aptamers' target were observed. In the case of the estradiol-binding aptamer and the adenosine-binding aptamer, Apt-AuNPs showed a higher tendency to aggregate after target-binding, as was expected based on other AuNP-based assays reported in the literature. Both, the riboflavin-binding aptamer and cholic acid-binding aptamer showed the opposite response, namely, that Apt-AuNPs became more stable upon target binding. The exact reason for this difference in response is not clear yet but seems to be due to specific aptamer-AuNPs interactions, probably related to the specific aptamer sequence and changes in its conformation in the unbound and bound state. The assays response characterization showed some cross-reactivity with non-target analytes. This cross-reactive nature of these Apt-AuNPs response was utilized to demonstrate for the first time a plasmonic multiplex sensor for small molecular targets. Principal components analysis was shown to cluster the data efficiently, allowing unambiguous analyte identification and quantification. This proof-of-concept work demonstrated that Apt-AuNPs can be utilized to design cross-reactive sensors for small molecular targets. This initial work in buffer systems opens the door to explore the utilization of the plasmonic response of Apt-AuNPs to design fast cross-reactive sensors for biologically relevant biomarkers. We envisioned that after optimization to improve the sensors sensitivity, coupling these detection systems to cell-phone based assay analysis will allow the use of these sensors in point of care diagnostics applications.

### Acknowledgements

## References

1. B. Duncan, S. G. Elci, V. M. Rotello, , *Nano Today,* 2012, 228-230
2. G. Poste, *Trends in Molecular Medicine,* 2012, **18**(12), 717-722
3. J. F. Rusling, *Anal. Chem*., 2013, **85**, 5304-5310
4. M. McKeague, and M. C. DeRosa, *Journal of Nucleic Acids,* 2012,Volume 2012, Article ID 748913
5. M. N. Stojanovic, and D. M. Kolpashchikov, *J. Am. Chem. Soc*., 2004, **126**, 9266-9270
6. O. R. Miranda, B. Creran, V. M. Rotello, *Current Opinion in Chemical Biology* 2010, **14**, 728-736
7. G. J. Worsley, S. L. Attree, J. E. Noble, A. M. Horgan, *Biosens. and Bioelectron*., 2012, **34**, 215-220
8. C-C. You, O.R. Miranda,B. Gider, P.S. Ghosh, I-B Kim, B. Erdogan, S. A. Krovi, U. H. F. Bunz, V. M. Rotello, *Nat. Nanotechnol*., 2007, **2**, 318-323
9. J. J. Lavigne, and E. V. Anslyn, *Angew., Chem. Int. Ed.,* 2001, **40**, 3118-3130
10. K. Saha, S. S. Agasti, C. Kim, X. Li, V. M. Rotello, *Chem. Rev.,* 2012, **112**, 2739-2779
11. K. L. Diehl, and E. V. Anslyn, *Chem. Soc. Rev.,* 2013, **42**, 8596-8611
12. N. O. Fisher, T. M. Tarasow, J.B-H. Toh, *Current Opinion in Chemical Biology* 2007, **11**, 316-328
13. M. Famulok and G. Mayer, *Accounts of Chemical Research* 2011, **44**(12), 1349-1358
14. A. B. Iliuk, L. Hu, W. A. Tao, *Anal. Chem*. 2011, **83**, 4440-4452
15. J. H. Lee, M. V. Yigit, D. Mazumdar, Y. Lu, *Advanced Drug Delivery Reviews,* 2010, **62**, 592-605
16. T. Kato, K. Yano, K. Ikebukuro, I. Karube, *Nucleic Acids Research,* 2000, **28**, 9, 1963-1968
17. M. N. Stojanovic, E. G. Green, S. Semova, D. B. Nikić, D. W. Landry, *J. Am. Chem. Soc*., 2003, **125**, 6085-6089
18. N. Derbyshire, S. J. White, D. H. J. Bunka, L. Song, S. Stead, J. Tarbin, M. Sharman, D. Zhou, P. G. Stockley, *Anal. Chem.*, 2012, **84**, 6595-6602
19. C. Rosman, J. Prasad, A. Neiser, A. Henkel, J. Edgar, C. Sönnichsen, *Nano Lett.,* 2013, **13**, 3243-3247
20. G. Wang, Y. Wang, L. Chen, J. Choo, *Biosens Bioelectron*. 2010, **25**, 1859-1868
21. F. Xia, X. Zuob, R. Yang, Y. Xiao, D. Kang, A. Vallée-Bélisle, X. Gong, J. D. Yuen, B. B. Y. Hsu, A. J. Heeger, K. W. Plaxco, *Proc. Natl. Acad. Sci U.S.A.*, 2010, **107**(24), 10837-10841
22. L. Wang, X. Liu, S. Song, C. Fan, *Chem. Commun*., 2006, 3780-3782
23. J. L. Chávez, W. Lyon, N. Kelley-Loughnane, M. O. Stone, *Biosens. Bioelectron*., 2010, **26**, 23-28
24. J. L. Chávez , R. I. MacCuspie, M. O. Stone, N. Kelley-Loughnane, *J. Nanopart. Res.,* 2012, **14**:1166
25. J. Liu, Y. Lu, *Angew Chem Int Ed,* 2006, **45**, 90-94
26. V. Pavlov, Y. Xiao, B. Shlyahovsky, I. Willner, , *J Am Chem Soc,* 2004,**126**, 11768-11769
27. H. Li, L. Rothberg, *Proc Natl Acad Sci USA,* 2004, **101**, 14036-14039
28. J. Zhang, L. Wang, D. Pan, S. Song, F. Y. C. Boey, H. Zhang, C. Fan, *Small* 2008, **8**, 1196-1200
29. J. E. Smith, D. K. Griffin, J. K. Leny, J. A. Hagen, J. L. Chávez, N. Kelley-Loughnane, *Talanta,* 2014, **121**, 247-255
30. U. H. F. Bunz, V.M. Rotello, *Angew. Chem. Int. Ed.,* 2010, **49**, 3268 – 3279
31. X. Li, F. Wen, B. Creran, Y. Jeong, X. Zhang, V. M. Rotello, *Small,* 2012, **8**, 3589-3592
32. Y. Lu, Y. Liu, S. Zhang, S. Wang, S. Zhang, X. Zhang, *Anal. Chem*., 2013, **85**, 6571-6574
33. C. Zhang, L. Wang, Z. Tu, X. Sun, Q. He, Z. Lei, C. Xu, Y. Liu, X. Zhang, J. Yang, X. Liu, Y. Xu, *Biosens. Bioelectron.,* 2014, **55**, 216-219
34. S. Pang, T. P. Labuzab, L. He, *Analyst,* 2014, **139**, 1895-1901
35. D. E. Huizenga, J. W. Szostak, *Biochemistry,* 1995, **34**, 656-665
36. C. T. Lauhon, J. W. Szostak, *J. Am. Chem. Soc.*, 1995, **117**, 1246-1257
37. Y. S. Kim, H. S. Jung, T. Matsuura, H-Y Lee, T. Kawai, M. B. Gu, Biosens. Bioelectron., 2007, **22**, 2525-2531
38. T. Kato, T. Takemura, K. Yano, K. Ikebukuro, I. Karube, *Biochimica et Biophysica Acta* 2000, **1493**, 12-18
39. V. Vallon, B. Muhlbauer, H. Osswald, Physiol. Rev. 86 (2006) 901-940
40. A. Gültekina, A. Ersözb, A Denizlic, R. Sayb, Sensors and Actuators B 162 (2012) 153– 158
41. P.N. Rao, E. Levine, M.O. Myers, V. Prakash, J. Watson, A. Stolier, J.J. Kopicko, P. Kissinger, S.G. Raj, M.H.G. Raj, Cancer Epidemiol Biomarkers Prev 1999, 8, 985-990
42. P. Viñas, N. Balsalobre, C, López-Erroz, M. Hernández-Córdoba, J. Agric. Food Chem. 2004, 52, 1789-1794
43. H. Wei, B. Li, J. Li, E. Wang, S. Dong, *Chem. Commun*., 2007, 3735–3737
44. M. Zheng, F. Davidson, X. Huang, *J. Am. Chem. Soc*., 2003, **125**, 7790-7791
45. S. H De Paoli Lacerda, J. J. Park, C. Meuse, D. Pristinski, M. L. Becker, A. Karim, J. F. Douglas, *ACS Nano,* 2010, **4**(1), 365-379
46. C. H. Lin, D. J. Patel, *Chemistry & Biology,* 1997, **4**(11), 817-832
47. M. A. D. Neves, O. Reinstein, P.E. Johnson, *Biochemistry,* 2010, **49**, 8478-8487
48. W. Zhao, W. Chiuman, J. C. F. Lam, S. A. McManus, W. Chen, Y. Cui, R. Pelton, M. A. Brook, Y. Li, *J Am Chem Soc,* 2008, **130**, 3610–3618

## Notes and references

*[a] Human Effectiveness Directorate, 711th Human Performance Wing, Air Force Research Laboratory, Wright-Patterson Air Force Base, OH 45433, United States,. Fax: XX XXXX XXXX; Tel: XX XXXX XXXX; E-mail: xxxx@aaa.bbb.ccc*

1
2
3
4
5
6
7
8
9
10
11
12
13
14
15
16
17
18
19
20
21
22
23
24
25
26
27
28
29
30
31
32
33
34
35
36
37
38
39
40
41
42
43
44
45
46
47
48
49
50
51
52
53
54
55
56
57
58
59
60

*[b] Current address: College of Engineering and Applied Science, School of Electronic and Computing Systems, University of Cincinnati, 812 Rhodes Hall, Cincinnati, OH 45221, United States*

*[c] Current address: College of Arts and Sciences, Department of*
5 *Chemistry and Biochemistry, Ohio State University, 1110 Newman and Wolfrom Laboratory, Columbus, OH 43210, United States*

‡ Footnotes should appear here. These might include comments relevant
15 to but not central to the matter under discussion, limited experimental and spectral data, and crystallographic data.
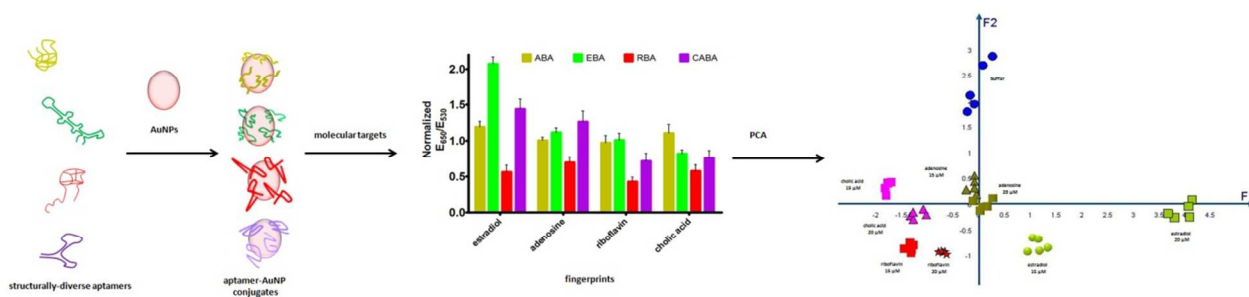
Apt-AuNPs were utilized as cross-reactive sensors for identification and quantification of small molecular targets through principal components analysis